

## Radio continuum and far-infrared emission from the galaxies in the Eridanus group

A. Omar\*<sup>†</sup> & K.S. Dwarkanath<sup>‡</sup>

*Raman Research Institute, Sadashivanagar, Bangalore 560 080, India*

Received xxx; accepted xxx

### Abstract.

The Eridanus galaxies follow the well-known radio-FIR correlation. Majority (70%) of these galaxies have their star formation rates below that of the Milky Way. The galaxies having a significant excess of radio emission are identified as low luminosity AGNs based on their radio morphologies obtained from the GMRT observations. There are no powerful AGNs ( $L_{20cm} > 10^{23} \text{ W Hz}^{-1}$ ) in the group. The two most far-infrared and radio luminous galaxies in the group have optical and H I morphologies suggestive of recent tidal interactions. The Eridanus group also has two far-infrared luminous but radio-deficient galaxies. It is believed that these galaxies are observed within a few Myr of the onset of an intense star formation episode after being quiescent for at least a 100 Myr. The upper end of the radio luminosity distribution of the Eridanus galaxies ( $L_{20cm} \sim 10^{22} \text{ W Hz}^{-1}$ ) is consistent with that of the field galaxies, other groups, and late-type galaxies in nearby clusters.

*Key words:* galaxy: radio continuum, radio-FIR correlation – galaxies: groups – individual: Eridanus

## 1. Introduction

There is a well-known correlation between the non-thermal radio emission and the thermal far-infrared (FIR) emission from star forming galaxies (van der Kruit 1973, Condon 1992, Yun, Reddy & Condon 2001). The radio-FIR correlation has been observed to be extremely tight ( $\sigma \sim 0.26$  dex)

---

\*Present address : ARIES, Manora peak, Nainital, 263 129, Uttaranchal, India

<sup>†</sup>e-mail: aomar@upso.ernet.in

<sup>‡</sup>e-mail: dwaraka@rri.res.in

over a wide range ( $10^9 - 10^{12} L_{\odot}$ ) of FIR luminosities (Yun, Reddy & Condon 2001). The origin and the tightness of the radio-FIR correlation is not completely understood. The radio-FIR correlation is linked to the star formation activities in galaxies, and is not displayed by Active Galactic Nuclei (AGNs). According to one scenario, ultra-violet photons from massive stars ( $M > 8 M_{\odot}$ ) heat the surrounding dust which emits in the far-infrared, and the same population of massive stars undergo supernova explosions thereby accelerating cosmic electrons responsible for much of the radio emission from galaxies (Harwit & Pacini 1975). The presence or absence of the correlation therefore can be used to make a distinction between the star formation and the AGN related radio continuum emission in galaxies.

The radio-FIR correlation has also been used to study the effects of environment on the evolution of radio sources in galaxy clusters and groups (e.g., Scodreggio & Gavazzi 1993, Gavazzi & Boselli 1999, Miller & Owen 2001, Menon 1995, Reddy & Yun 2004). Studies indicate that normal star forming galaxies in the local Universe seldom have their 20 cm spectral luminosities exceeding  $10^{23} \text{ W Hz}^{-1}$ , but AGNs are observed with higher radio luminosities (Condon 1989, Yun, Reddy & Condon 2001). Studies in clusters of galaxies indicate that the luminous radio AGNs ( $L_{20\text{cm}} > 10^{23} \text{ W Hz}^{-1}$ ) are hosted mostly by early type galaxies in the cores of clusters (e.g., Gavazzi & Boselli 1999, Reddy & Yun 2004). These radio-luminous AGNs are more commonly found in the cluster environment than in the field. These studies indicate that the upper end of the radio luminosity distribution of late type galaxies does not differ much in different environments.

The Eridanus group was recently studied in detail (Omar 2004, Omar & Dwarakanath 2004a,b). This group has  $\sim 200$  identified members. This group was predicted to be in an early phase of the cluster formation where different sub-groups are merging together (Willmer et al. 1989). Although the entire group is not dynamically relaxed, the galaxy evolution process seems to be effective in the group. A significant H I deficiency up to a factor of 2 – 3 was observed in the Eridanus galaxies in the high galaxy density regions (Omar & Dwarakanath 2004b). This group also has a significantly large (30%) population of early types (E+S0's). In this paper, the radio-FIR correlation for the Eridanus galaxies is constructed using the FIR data from the *Infrared Astronomical Satellite* (IRAS; Neugebauer et al. 1984) survey and the 20 cm radio data from the *Northern VLA Sky Survey* (NVSS; Condon et al. 1998). The higher resolution ( $5'' - 10''$ ) radio continuum images at 20 cm from the GMRT observations are used to study the nature of the galaxies departing from the radio-FIR correlation. The GMRT radio continuum images of some of the normal star forming galaxies are also presented.

## 2. The FIR and the radio data

### 2.1 The IRAS data

The IRAS faint source catalog has a limiting sensitivity of  $\sim 0.3$  Jy at  $\lambda 60\mu$ . The  $60\mu$  flux density,  $S_{60\mu}$  is converted to the luminosity,  $L_{60\mu}$  using the relation:

$$\log \frac{L_{60\mu}}{L_{\odot}} = 6.014 + 2 \log \frac{D}{\text{Mpc}} + \log \frac{S_{60\mu}}{\text{Jy}} \quad (1)$$

At the distance to the Eridanus group ( $D \sim 23$  Mpc), the limiting sensitivity of the *IRAS* observations is  $L_{60\mu} \sim 10^8 L_{\odot}$ . The total FIR luminosity,  $L_{\text{FIR}}$  is estimated using the relation (Helou et al. 1998):

$$L_{\text{FIR}}(L_{\odot}) = \left( 1 + \frac{S_{100\mu}}{2.58 S_{60\mu}} \right) L_{60\mu} \quad (2)$$

### 2.2 The NVSS data

The 20 cm flux densities are from the NVSS made at a resolution of  $45''$  ( $\sim 5$  kpc) with an rms of  $0.5$  mJy beam $^{-1}$ . The 20 cm spectral luminosity,  $L_{20\text{cm}}$  is estimated using the relation:

$$\log \frac{L_{20\text{cm}}}{\text{WHz}^{-1}} = 20.08 + 2 \log \frac{D}{\text{Mpc}} + \log \frac{S_{20\text{cm}}}{\text{Jy}} \quad (3)$$

The  $5\sigma$  sensitivity to the 1.4 GHz spectral luminosity is  $\sim 1.6 \times 10^{20}$  W Hz $^{-1}$ .

### 2.3 The GMRT observations

A total of 57 galaxies in the Eridanus group were observed by Omar & Dwarkanath (2004a) using the GMRT. The observing strategy was optimized to get uniform distribution of visibilities. Two galaxies were observed alternately for 15 – 20 minutes each followed by 5 – 7 minutes of observations of the secondary calibrators. This cycle was repeated and a total of 3–4 hour of observing time was accumulated on each galaxy. Majority of these observations were carried out over a bandwidth of 8 MHz divided into 128 spectral channels. These observations were primarily aimed at detecting H I emission from the Eridanus galaxies. No pre-selection of galaxies was made based on their radio or optical properties. Both early type and late type galaxies were observed. The data were corrected for the spectral response of the IF filters. The channels devoid of H I line signals were averaged to obtain the radio continuum data. The GMRT has a mix of both short and long baselines which make the data sensitive to extended emission and at the same time also make it possible to obtain a high resolution image.

**Table 1.** GMRT image parameters

| <b>Galaxy</b> | <b>rms</b><br>(mJy/bm) | <b>Resolution</b><br>(arc sec) | <b>S<sub>total</sub></b><br>(mJy) | <b>Morph.</b> |
|---------------|------------------------|--------------------------------|-----------------------------------|---------------|
| NGC 1407      | 0.50                   | 6 × 6                          | 99 ± 10                           | Diffuse       |
| NGC 1371      | 0.22                   | 15 × 15                        | 19.7 ± 2                          | Linear        |
| NGC 1415      | 0.12                   | 4 × 4                          | 27 ± 3                            | Linear        |
| NGC 1482      | 0.81                   | 8 × 8                          | 280 ± 30                          | Diffuse       |
| NGC 1385      | 0.41                   | 15 × 15                        | 180 ± 20                          | Diffuse       |
| NGC 1377      | 0.20                   | 15 × 15                        | < 1 (5σ)                          | –             |
| IC 1953       | 0.30                   | 50 × 45                        | 9 ± 2                             | Diffuse       |
| NGC 1309      | 0.35                   | 15 × 15                        | 68 ± 7                            | Diffuse       |
| NGC 1345      | 0.23                   | 32 × 26                        | 4.5 ± 1                           | Diffuse       |
| ESO 548-G 036 | 0.20                   | 16 × 11                        | 9 ± 1                             | Diffuse       |

Notes: Images are natural-weighted. The resolution of each image is such that the diffuse emission is emphasized without losing much of the resolution.

The data were analysed following the standard procedures using the *Astronomical Image Processing System* (AIPS) developed by the National Radio Astronomy Observatory (NRAO). The flux density scale of these observations is based on the standard VLA calibrators 3C 48 and 3C 147. Images were CLEANed and self-calibrated to improve the dynamic range. The images presented here are at angular resolutions which emphasize the extended radio continuum emission from the galaxies. The details of the image properties are given in Tab. 1. The total flux densities are estimated from images at a resolution of  $\sim 1'$ . The GMRT flux densities are consistent with the NVSS flux densities within 20% for most of the galaxies except for the two weaker ones, viz., IC 1953 and ESO 548- G 036 where the uncertainties are 25% and 30% respectively.

### 3. The Radio and FIR emission from the Eridanus galaxies

A total of 72 Eridanus galaxies are detected in the IRAS survey, out of which 38 galaxies were detected in the NVSS. A total of 7 early type (E+S0's) galaxies are detected in radio, most of them being radio weak ( $L_{20cm} \sim 10^{20} \text{ W Hz}^{-1}$ ). The list of Eridanus galaxies detected in the FIR and in the radio is given in Table 2. The histograms of the radio and the FIR luminosities of the galaxies in the Eridanus group are plotted in Fig. 1. The Eridanus galaxies have their radio spectral luminosities below  $\sim 10^{22} \text{ W Hz}^{-1}$ . The high end of the radio luminosity of the galaxies in the Hickson compact groups (Menon 1995) and the Ursa-Major group (Verheijen & Sancisi 2001) is consistent with that in the Eridanus galaxies. Majority of

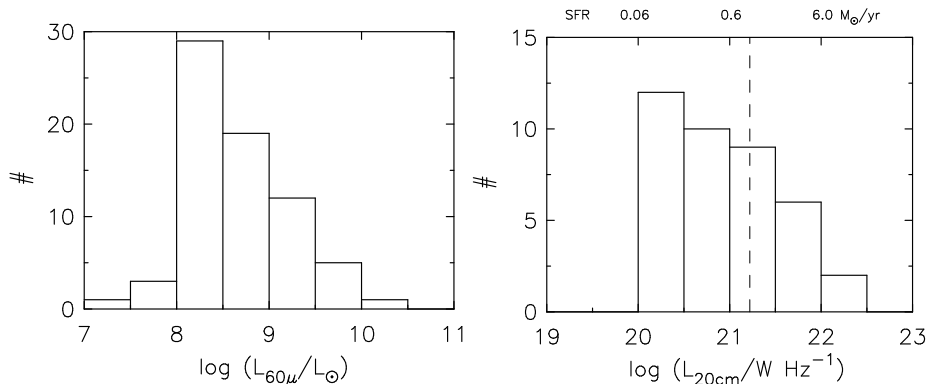


**Figure 1.** Histograms of radio and FIR luminosities of the Eridanus galaxies. The dashed vertical line in the right hand side panel corresponds to the star formation rate of the Milky-way.

the late-type galaxies in nearby clusters also have their radio luminosities below  $\sim 10^{22}$   $\text{W Hz}^{-1}$  (Reddy & Yun 2004). It is interesting to observe that the groups (Ursa-Major, HCG's, and Eridanus) lack in powerful AGNs ( $L_{20\text{cm}} > 10^{23}$   $\text{W Hz}^{-1}$ ), which are more commonly associated with the early-type galaxies in clusters (Reddy & Yun 2004). It can also be noticed from Fig. 1 that majority ( $\sim 70\%$ ) of the Eridanus galaxies have their star formation rates below that of the Milky Way ( $\sim 1 \text{ M}_{\odot} \text{ yr}^{-1}$ ).

#### 4. The Radio-FIR correlation

The radio-FIR correlation for the Eridanus galaxies is shown in Fig. 2. The  $5\sigma$  upper limits ( $\log(L_{20\text{cm}}/\text{W Hz}^{-1}) \sim 20.2$ ) for the non-detections in radio are marked by arrows. The sample size for the Eridanus galaxies is relatively small, and does not span a large range of infrared luminosity. Therefore, any fit is of little statistical importance. The best fit straight line for the radio-FIR correlation obtained by Yun, Reddy & Condon (2001) on a large sample of IRAS galaxies is shown in Fig. 2. This straight line corresponds to a slope of 1 and an intercept of 12.07. It can be seen that majority of the Eridanus galaxies follow the radio-FIR correlation.

Following Condon, Anderson & Helou (1991), the  $q$  parameter is plotted for the Eridanus galaxies in Fig 3. The  $q$  parameter is estimated using the following relation:

$$q = \log\left(\frac{2.58S_{60\mu} + S_{100\mu}}{2.98 \text{ Jy}}\right) - \log\left(\frac{S_{20\text{cm}}}{\text{Jy}}\right) \quad (4)$$

In Fig. 3, the two dotted lines mark three times radio excess (below the mean) and three time FIR excess (above the mean) respectively. The mean

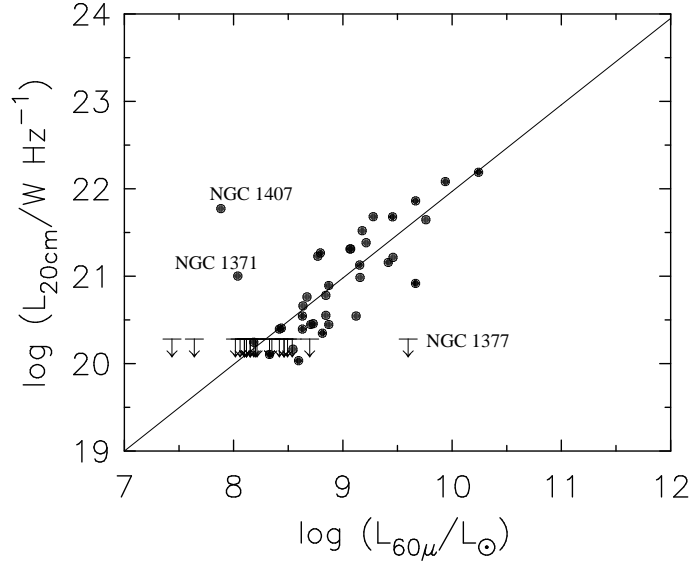


**Figure 2.** The radio-FIR correlation for the galaxies in the Eridanus group using the data from IRAS and NVSS. The straight line is not a fit to the data. It is the best fit obtained by Yun, Reddy & Condon (2001) for an all-sky sample of infrared detected galaxies from IRAS.

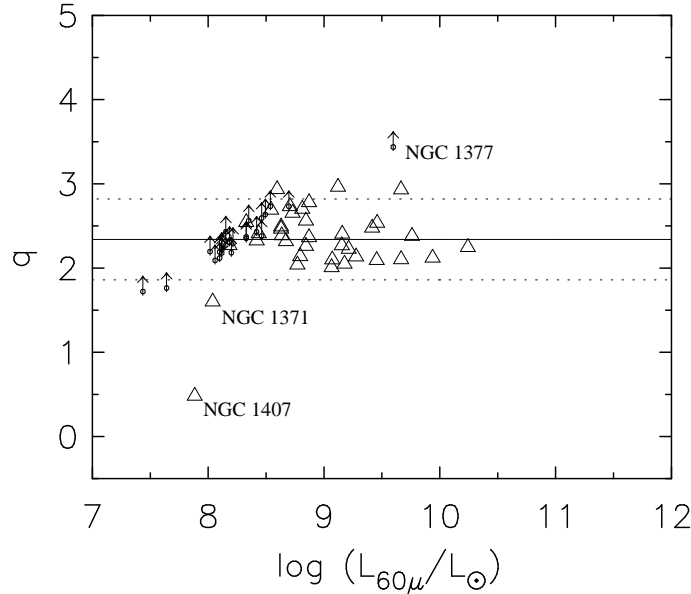


**Figure 3.** The  $q$  parameter for the Eridanus galaxies. The solid line is at  $q = 2.34$  which is the mean value obtained by Yun, Reddy & Condon (2001), and is not a fit for the present data. The top and the bottom dotted lines are limits for three times FIR excess and three times radio excess from the mean respectively.

value shown by the solid line is at  $q = 2.34$  as obtained by Yun, Reddy & Condon (2001).

It can be noticed from Figs. 2 and 3 that there are some galaxies which deviate significantly (more than 3 times) from the mean radio-FIR correlation. Rest of the galaxies follow the radio-FIR correlation within an rms of 0.47 dex (Fig. 2). A significant deviation in the  $q$  value can be noticed at FIR luminosities below  $10^9 L_{\odot}$ . Such trends are known from earlier studies (e.g., Condon, Anderson & Helou 1991, Yun et al. 2001). It is believed that this non-linearity is due to the heating of dust from the old stellar population in galaxies (Condon, Anderson & Helou 1991). The FIR emission due to this heating is insignificant compared to that due to heating from massive stars in normal star forming galaxies.

## 5. The Radio-excess galaxies

The two Eridanus galaxies, viz., NGC 1407 and NGC 1371 have significant radio excesses. These two galaxies are marked in Fig. 3 (also, see Table 3). The radio emission in excess of that expected from the mean radio-FIR correlation may be due to an AGN in the galaxy. The radio continuum emission from AGNs is often from a nuclear point source or a pair of jets or from both. The GMRT radio continuum contour images of these two galaxies are shown in Fig. 4 overlaid upon their respective optical images from the DSS. It can be noticed that both the galaxies have kpc-scale linear radio structures in their respective centres. Such a feature is indicative of an AGN. A description of these two galaxies is given below.

### 5.1 NGC 1407 (E0)

NGC 1407 has more than 70 times excess radio emission compared to that expected from the radio-FIR correlation. It is the most optically luminous ( $L_B = 4 \times 10^{10} L_{\odot}$ ) galaxy in the Eridanus group. It resides in a sub-group having a morphological mix of 70% (E+S0's) and 30% (Sp+Irr's) which is similar to those in galaxy clusters. NGC 1407 has a nuclear X-ray source. Diffuse X-ray emission is also seen in the Intra-group medium surrounding the galaxy (Omar & Dwarakanath 2004a). This galaxy was not detected in HI ( $M_{\text{HI}} (5\sigma) < 1.2 \times 10^7 M_{\odot}$ ). No HI absorption was detected toward the radio source down to a  $5\sigma$  optical depth limit of 0.05.

The GMRT radio continuum morphology (Fig. 4) shows diffuse emission along a linear structure and a nuclear continuum source coincident with the X-ray nuclear source. The X-ray and radio nucleus, a linear radio structure, and the large radio-excess suggest the presence of an AGN in this galaxy.

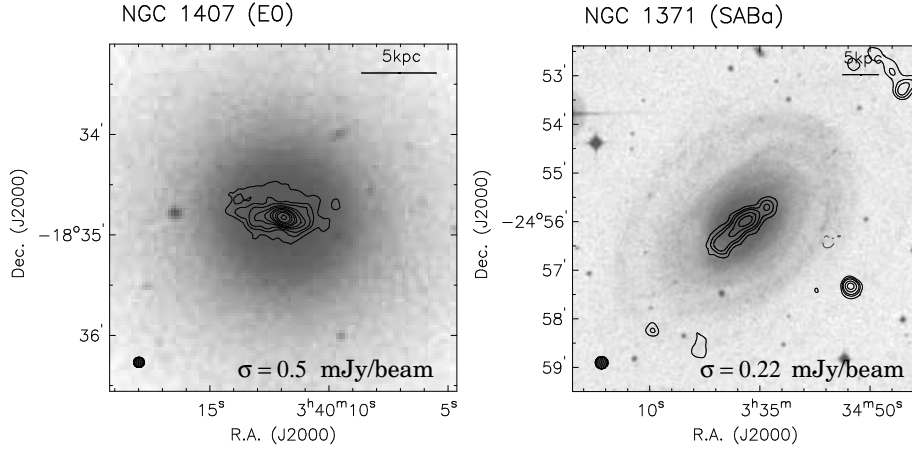


**Figure 4.** The contours of the radio continuum emission from the radio-excess galaxies in the Eridanus group observed with the GMRT are overlaid upon their respective optical images from the DSS. The contours start at 3 times the rms value ( $\sigma$ , indicated in the map) and increases in steps of 4.5, 6, 9, 12, 18, 24, 36, 48,  $72 \times \sigma$ .

## 5.2 NGC 1371 (SABa)

NGC 1371 has more than 5 times excess radio emission compared to that expected from the radio-FIR correlation. It is among one of the largest ( $D_{B25} \sim 38$  kpc) galaxies in the Eridanus group. The optical luminosity ( $L_B = 2 \times 10^{10} L_\odot$ ) is dominated by the bulge. It has faint spiral arms in the outer regions. The galaxy was observed in  $H\alpha$  by Hameed & Devereux (1999). The  $H\alpha$  image shows emission from HII regions in the spiral arms, weak diffuse emission in the bulge, a nuclear source and a ring-like structure surrounding the nucleus. The GMRT radio continuum morphology (Fig. 4) shows kpc-scale linear jet like structure and a bright radio source coincident with the  $H\alpha$  nuclear source. No  $H\alpha$  emission is seen corresponding to the extended radio emission. Therefore, it is unlikely that the extended radio emission is due to the star formation activities, and could be due to a radio jet. The radio morphology, the presence of a nuclear point source in radio and in  $H\alpha$  and a significant radio excess indicate an AGN in this galaxy. The apparent alignment of the linear radio structure with the major axis of NGC 1371 is likely to be due to a projection effect although in reality the jet may be at a considerable angle from the plane of the galaxy.

## 6. The Normal star-forming galaxies

The majority (70%) of galaxies in the Eridanus group have their star formation rates (SFR) below that of the Milky Way, viz.,  $\sim 1 M_\odot \text{ yr}^{-1}$ . The

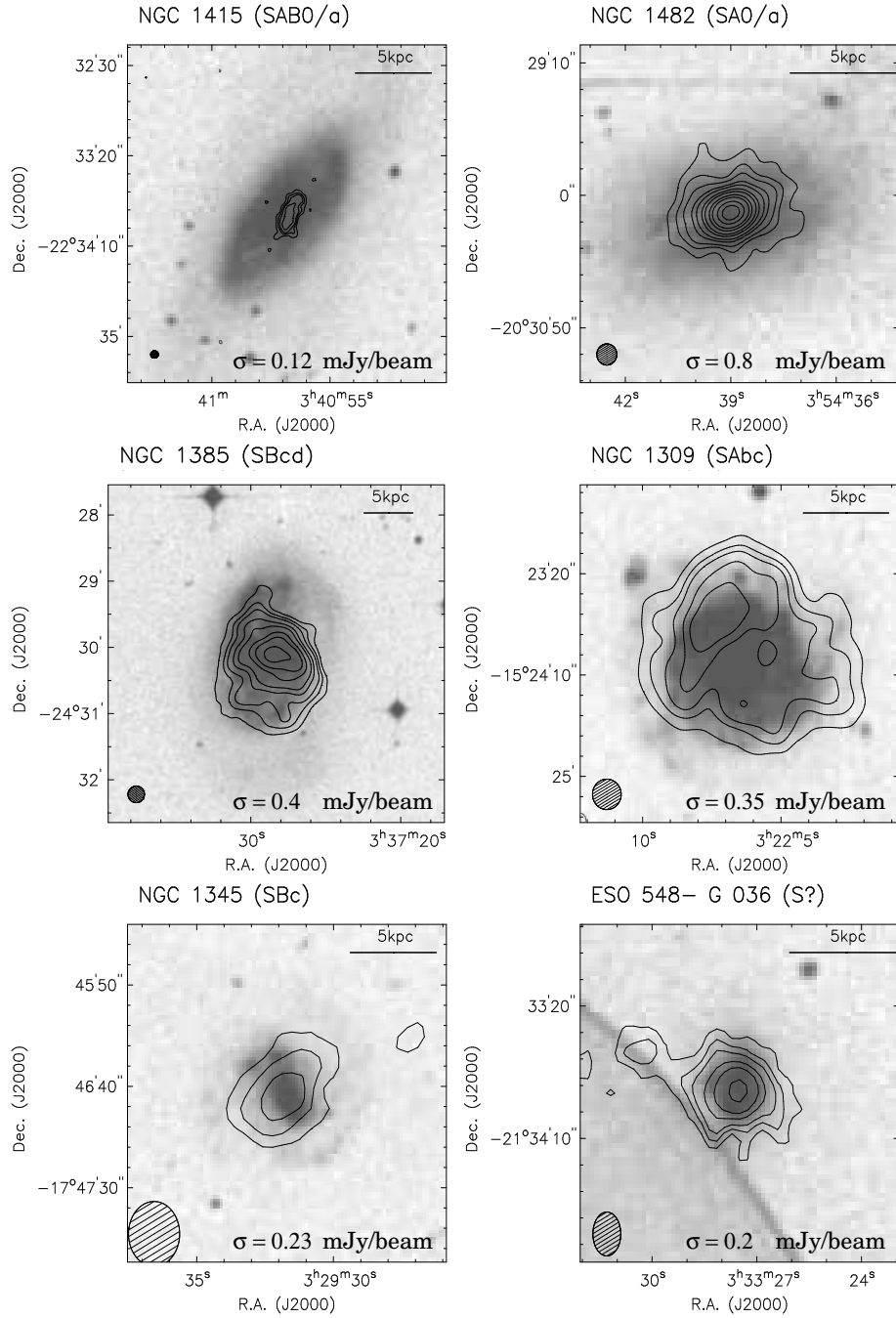


**Figure 5.** GMRT radio continuum images (in contours) of some of the normal star forming galaxies in the Eridanus group overlaid upon their respective optical images from the DSS (see Table 3). The contour levels are similar to Fig. 4. The rms values of the respective images are indicated in each image.

SFR can be inferred from the FIR luminosity or from the radio luminosity. The SFR ( $\alpha$ ) can be estimated from the FIR flux densities using the relation (Kennicutt 1998):

$$\alpha = 1.7 \times 10^{-10} f (1 + 0.387 S_{100\mu m} / S_{60\mu m}) L_{60\mu m} \quad (5)$$

The value of  $f$  is quite uncertain and varies in the range 1.2 – 2 for star-burst galaxies (Sanders, Scoville & Soifer 1991).

The value of  $\alpha$  can be estimated using the 20 cm radio spectral luminosity (Yun et al. 2001):

$$\alpha \sim 6 \times 10^{-22} \frac{L_{20cm}}{W Hz^{-1}} \quad (6)$$

The radio continuum images of some of the normal star forming galaxies in the Eridanus group are shown in Fig 5. The radio emission is diffuse in these galaxies. It can be seen that the radio continuum emission in NGC 1309 and NGC 1385 follows the spiral arms. This is a common trend observed in spiral galaxies where it is believed that the spiral density wave compresses the magnetic field in the spiral arms thereby increasing the magnetic field strength and hence the synchrotron emission.

The most FIR luminous galaxies in the group are NGC 1482 ( $L_{FIR} \sim 4.3 \times 10^{10} L_{\odot}$ ) and NGC 1385 ( $L_{FIR} \sim 2.5 \times 10^{10} L_{\odot}$ ). Although these galaxies are 'star-bursts' (Table 3), they are called 'normal' since they follow the radio-FIR correlation. Both of these galaxies have signatures of recent tidal interactions in their optical images. NGC 1385 (SBcd) has a faint stellar envelop to the south and disturbed spirals arms. NGC 1482 (SA0) has faint stellar streamers surrounding it. The H I tidal tails were detected in NGC 1482 (Omar & Dwarakanath 2004b). The large amounts ( $M_{H_2} \sim 10^9 M_{\odot}$ ) of molecular Hydrogen in the centres of these two galaxies have been inferred from the CO observations (Sanders, Scoville & Soifer 1991, Elfhag et al. 1996). Strong stellar winds indicative of a star-burst were detected in H $_{\alpha}$  (Hameed & Devereux 1999, Veilleux & Rupke 2002).

## 7. The FIR-excess (radio-deficient) galaxies

Galaxies having significant excess FIR emission are not common. Yun, Reddy & Condon (2001) noticed 9 galaxies with  $q$  value greater than 3 in a sample of nearly 1800 galaxies. A significantly higher  $q$  value implies that the galaxy has excess FIR emission than expected from the radio luminosity. Galaxies with  $L_{60\mu} \sim 10^8 L_{\odot}$  are likely to have excess FIR emission due to the heating of dust from the old stellar population (Condon, Anderson & Helou 1991). These galaxies are not considered here. The nine FIR excess galaxies of Yun, Reddy & Condon (2001) have  $L_{60\mu} > 10^9 L_{\odot}$ . The FIR excess in these galaxies was diagnosed recently by Roussel et al. (2003)

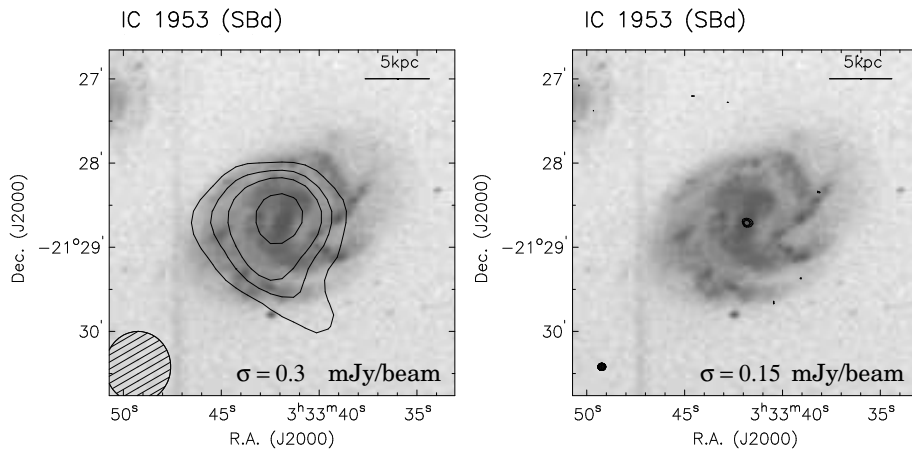


**Figure 6.** The GMRT radio continuum morphologies (in contours) of IC 1953 at resolutions of  $50'' \times 45''$  (left) and  $5'' \times 5''$  (right) overlaid on the optical image from the DSS. The contours are at  $0.9, 1.4, 1.8$  and  $2.7 \text{ mJy beam}^{-1}$  for the lower resolution image and  $0.5, 0.7,$  and  $0.9 \text{ mJy beam}^{-1}$  for the higher resolution image.

who showed that these galaxies are most likely observed within a few Myr of the onset of an intense star formation episode after being quiescent for at least 100 Myr. According to them, this star-burst, while heating the dust, has not produced cosmic rays yet. Therefore, these galaxies are radio-deficient. Such galaxies must be rare to be observed at a given epoch since the typical ages of massive stars ( $\sim 1 \text{ Myr}$ ) are only a small fraction of the ages of the star-bursts ( $\sim 100 \text{ Myr}$ ) in galaxies. The actual number of such synchrotron deficient galaxies will depend further on the time intervals of successive star-burst events in a galaxy.

The Eridanus group has two such galaxies, viz., NGC 1377 and IC 1953. Both these galaxies were studied by Roussel et al. (2003). The  $q$  values are  $\sim 3.4$  for NGC 1377 and  $\sim 2.9$  for IC 1953. These two galaxies are marked in Fig. 3. A brief description of these two galaxies is given below.

### 7.1 NGC 1377 (S0)

NGC 1377 is FIR luminous ( $L_{FIR} = 8 \times 10^9 L_{\odot}$ ) with  $S_{60\mu}/S_{100\mu} \sim 1.3$  indicating the presence of warm dust in the galaxy. The warm IRAS galaxies are believed to be due to nuclear star-burst probably triggered by recent interactions or mergers (Heisler & Vader 1995). The radio continuum emission from this galaxy is not detected in the GMRT image down to a  $5\sigma$  sensitivity limit of  $1 \text{ mJy}$ . NGC 1377 is, therefore, radio deficient by at least 40 times.

## 7.2 IC 1953 (SBd)

IC 1953 has grand spiral arms and a prominent bar. The radio continuum morphology consists of diffuse emission from the disk and a nuclear point source (Fig. 6). Using high resolution (kpc-scale) mid-infrared images from ISO (Infrared Space Observatory) observations and high resolution radio continuum images from the VLA observations, Roussel et al. (2003) showed that while the disk radio continuum emission in IC 1953 is consistent with the disk infrared emission, the nuclear radio emission is not. According to them, it is suggestive of a recent nuclear star-burst.

## 8. Conclusions

- The upper end of the radio luminosity distribution of the Eridanus galaxies ( $L_{20cm} \sim 10^{20}$  W Hz $^{-1}$ ) is consistent with that of field galaxies, other groups, and late-type galaxies in clusters of galaxies.
- The Eridanus group lacks powerful AGNs ( $L_{20cm} > 10^{23}$  W Hz $^{-1}$ ) commonly found in rich clusters.
- Most of the Eridanus galaxies follow the well-known radio-FIR correlation.
- Majority ( $\sim 70\%$ ) of the Eridanus galaxies have their SFR below that of the Milky Way.
- Two previously unknown low luminosity AGNs ( $L_{20cm} < 10^{22}$  W Hz $^{-1}$ ) have been detected in the group.
- The most FIR and radio luminous galaxies in the Eridanus group have their optical and HI morphologies suggestive of recent tidal interactions.
- The Eridanus group has two FIR luminous ( $L_{FIR} \sim 10^{10} L_{\odot}$ ) but radio-deficient galaxies. It is believed that these galaxies are most likely observed within a few Myr of the onset of an intense star formation episode after being quiescent for at least 100 Myr.

## Acknowledgments

We thank the staff of the GMRT who made these observations possible. The GMRT is operated by the National Centre for Radio Astrophysics of the Tata Institute of Fundamental Research. This research has made use of the NASA/IPAC Infrared archived data and Northern VLA Sky Survey data. This research has been benefited by the NASA's Astrophysics Data System (ADS) and Extra-galactic Database (NED) services.

## References

- Condon, J.J. 1989, *Astrophys. J.*, **338**, 13
- Condon, J.J., Anderson, M.L., & Helou, G. 1991, *Astrophys. J.*, **376**, 95
- Condon, J.J. 1992, *Ann. Rev. Astron. Astrophys.*, **30**, 575
- Condon, J.J., Cotton, W. D., Greisen, E. W. et al. 1998, *Astron. J.*, **115**, 1693
- Elfhag, T., Booth, R.S., Hoeglund, B. et al. 1996, *Astron. Astrophys. Supl.*, **115**, 439
- Gavazzi, G., & Boselli, A. 1999, *Astron. Astrophys.*, **343**, 93
- Helou, G., Khan, I.R., Malek, L., & Boehmer, L. 1988, *Astrophys. J. Supl.*, **68**, 151
- Hameed, S., & Devereux, N. 1999, *Astron. J.*, **118**, 730
- Harwit, M., & Pacini, F. 1975, *Astrophys. J. Letters*, **200**, 127
- Heisler, C.A., & Vader, J.P. 1995, *Astron. J.*, **110**, 87
- Kennicutt, R.C. 1998, *Ann. Rev. Astron. Astrophys.*, **36**, 189
- Menon T. K. 1995, *Mon. Not. R. Astron. Soc.*, **274**, 845
- Miller, N., & Owen, F.N 2001, *Astron. J.*, *121*, 1903
- Neugebauer, G. et al. 1984, *Astrophys. J. Letter*, **278**, 1
- Omar, A. 2004, *Ph.D. thesis, Jawaharlal Nehru University, Delhi*
- Omar A. & Dwarakanath, K. S. 2004a, *J. Astrophys. Astron.*, this volume
- Omar A. & Dwarakanath, K. S. 2004b, *J. Astrophys. Astron.*, this volume
- Reddy, N.A. & Yun, M.S. 2004, *Astrophys. J.*, **600**, 695
- Roussel, H., Helou, G., Beck, R. et al. 2003, *Astrophys. J.*, **593**, 733
- Sanders, D.B., Scoville, N.Z., & Soifer, B.T. 1991, *Astrophys. J.*, **370**, 158
- Scodeggio, M., & Gavazzi, G. 1993, *Astrophys. J.*, **409**, 110
- van der Kruit, P.C. 1973, *Astron. Astrophys.*, **29** 263
- Veilleux, S., & Rupke, D. S. 2002, *Astrophys. J. Letter*, **565**, 63
- Verheijen, M.A.W., & Sancisi, R. 2001, *Astron. Astrophys.*, **370**, 765
- Willmer, C.N.A., Focardi, P., da Costa, L.N., & Pellegrini, P.S. 1989, *Astron. J.*, **98**, 1531
- Yun, M.S., Reddy, N.A., & Condon, J.J. 2001, *Astrophys. J.*, **554**, 803

**A. Table : FIR and radio continuum properties of the Eridanus galaxies**

The description of the table columns of Tab. 2 are as follows:

*Column 1* : Name of the galaxy.

*Column 2* : Hubble type.

*Column 3* :  $60\mu$  flux density from IRAS.

*Column 4* :  $100\mu$  flux density from IRAS.

*Column 5* : Total FIR luminosity using Equ. 2.

*Column 6* : 20 cm flux density from *NVSS*.

*Column 7* : 20 cm spectral luminosity using Equ. 3.

*Column 8* : Star formation rate using Equ. 6.

**Table 2.** FIR and radio properties of Eridanus galaxies

| Name            | H.T.   | S <sub>60μ</sub><br>(Jy) | S <sub>100μ</sub><br>(Jy) | log $\frac{L_{FIR}}{L_{\odot}}$ | S <sub>20cm</sub><br>(mJy) | log $\frac{L_{20cm}}{WHz^{-1}}$ | SFR<br>(M <sub>⊙</sub> /yr) |
|-----------------|--------|--------------------------|---------------------------|---------------------------------|----------------------------|---------------------------------|-----------------------------|
| NGC 1300        | Sbbc   | 2.75                     | 10.3                      | 9.77                            | 52.1                       | 21.52                           | 1.96                        |
| UGCA 068        | SABm   | 0.21                     | 0.56                      | 8.57                            | –                          | < 20                            | < 0.06                      |
| NGC 1325        | SAbc   | 0.63                     | 3.21                      | 9.21                            | –                          | < 20                            | < 0.06                      |
| NGC 1325A       | SBbc   | 0.24                     | 0.85                      | 8.70                            | –                          | < 20                            | < 0.06                      |
| NGC 1332        | S0     | 0.50                     | 1.78                      | 9.02                            | 4.0                        | 20.40                           | 0.15                        |
| NGC 1345        | SBc    | 0.78                     | 1.59                      | 9.06                            | 3.9                        | 20.40                           | 0.15                        |
| NGC 1347        | ?      | 0.30                     | 0.99                      | 8.78                            | –                          | < 20                            | < 0.06                      |
| ESO 548- G 028  | SB0    | 0.29                     | 0.61                      | 8.66                            | –                          | < 20                            | < 0.06                      |
| ESO 548- G 029  | SB ?   | 0.24                     | 0.73                      | 8.66                            | –                          | < 20                            | < 0.06                      |
| NGC 1353        | SAbc   | 2.42                     | 8.79                      | 9.70                            | 5.5                        | 20.54                           | 0.21                        |
| IC 1952         | SBbc   | 0.79                     | 3.19                      | 9.25                            | 7.2                        | 20.66                           | 0.27                        |
| IC 1953         | SBd    | 8.47                     | 11.28                     | 10.05                           | 13.0                       | 20.92                           | 0.49                        |
| NGC 1359        | SBm    | 2.13                     | 4.28                      | 9.52                            | 32.2                       | 21.31                           | 1.21                        |
| ESO 548- G 047  | SB0    | 0.39                     | 1.00                      | 8.83                            | –                          | < 20                            | < 0.06                      |
| NGC 1370        | E+     | 1.19                     | 2.17                      | 9.25                            | 3.5                        | 20.35                           | 0.13                        |
| NGC 1377        | S0     | 7.25                     | 5.74                      | 9.92                            | –                          | < 20                            | < 0.06                      |
| NGC 1385        | SBcd   | 15.87                    | 33.78                     | 10.40                           | 190                        | 22.08                           | 7.13                        |
| NGC 1395        | E2     | 0.05                     | 0.34                      | 8.20                            | –                          | < 20                            | < 0.06                      |
| NGC 1400        | S0     | 0.72                     | 2.50                      | 9.17                            | 1.7                        | 20.03                           | 0.06                        |
| NGC 1407        | E0     | 0.14                     | 0.48                      | 8.45                            | 93.3                       | 21.77                           | 3.50                        |
| NGC 1415        | SAB0/a | 5.27                     | 12.73                     | 9.95                            | 25.8                       | 21.22                           | 0.97                        |
| ESO 482- G 035  | SBab   | 0.26                     | 1.00                      | 8.75                            | –                          | < 20                            | < 0.06                      |
| NGC 1422        | SBab   | 0.39                     | 1.09                      | 8.85                            | –                          | < 20                            | < 0.06                      |
| NGC 1439        | E1     | –                        | 0.34                      | –                               | –                          | –                               | < 20                        |
| NGC 1440        | SB0    | –                        | 1.29                      | –                               | –                          | –                               | < 20                        |
| NGC 1438        | SB0/a  | 0.23                     | 0.79                      | 8.67                            | –                          | < 20                            | < 0.06                      |
| NGC 1481        | SA0    | 0.36                     | –                         | 8.50                            | 3.7                        | 20.37                           | 0.14                        |
| ESO 548- G 036  | S?     | 1.94                     | –                         | 9.23                            | 7.4                        | 20.67                           | 0.28                        |
| ESO 548- G 043  | Sa     | 0.35                     | –                         | 8.49                            | –                          | < 20                            | < 0.06                      |
| UGCA 073        | E+     | 0.3                      | –                         | 8.42                            | –                          | < 20                            | < 0.06                      |
| NGC 1145        | Sc     | 0.98                     | 3.50                      | 9.31                            | 4.5                        | 20.46                           | 0.17                        |
| NGC 1163        | SBbc   | 0.64                     | 1.71                      | 9.06                            | 2.3                        | 20.17                           | 0.09                        |
| MCG -03-08-057  | SAd    | 0.57                     | 2.39                      | 9.12                            | –                          | < 20                            | < 0.06                      |
| NGC 1187        | SBc    | 10.54                    | 22.41                     | 10.22                           | 69.6                       | 21.65                           | 2.61                        |
| NGC 1179        | SBd    | 0.41                     | 2.21                      | 9.04                            | –                          | < 20                            | < 0.06                      |
| NGC 1231        | Sc     | 0.23                     | 0.58                      | 8.60                            | –                          | < 20                            | < 0.06                      |
| MRK 1069        | ?      | 1.28                     | 1.86                      | 9.24                            | 9.5                        | 20.78                           | 0.36                        |
| NGC 1232        | SABc   | 3.47                     | 21.7                      | 10.02                           | 75.5                       | 21.68                           | 2.83                        |
| IC 1898         | SBc    | 0.78                     | 2.77                      | 9.21                            | 5.5                        | 20.54                           | 0.21                        |
| NGC 1255        | SABbc  | 2.99                     | 11.36                     | 9.81                            | 38.0                       | 21.38                           | 1.43                        |
| NGC 1258        | SABcd  | 0.28                     | 1.09                      | 8.79                            | –                          | < 20                            | < 0.06                      |
| NGC 1292        | SAc    | 1.36                     | 4.38                      | 9.43                            | 4.4                        | 20.45                           | 0.17                        |
| UGCA 064        | SBcd   | 0.19                     | 0.91                      | 8.68                            | –                          | < 20                            | < 0.06                      |
| NGC 1302        | SABa   | 0.26                     | 1.74                      | 8.91                            | –                          | < 20                            | < 0.06                      |
| NGC 1306        | Sb     | 2.63                     | 4.73                      | 9.59                            | 15.2                       | 20.99                           | 0.57                        |
| IRAS 03191 2456 | S0     | 0.53                     | 0.78                      | 8.86                            | –                          | < 20                            | < 0.06                      |

|                 |       |       |       |       |       |       |        |
|-----------------|-------|-------|-------|-------|-------|-------|--------|
| NGC 1309        | SAbc  | 5.22  | 14.26 | 9.97  | 75.2  | 21.68 | 2.82   |
| UGCA 071        | Sd    | 0.28  | 0.81  | 8.71  | 2.76  | 20.24 | 0.10   |
| NGC 1338        | SABb  | 1.36  | 4.95  | 9.46  | 12.3  | 20.89 | 0.46   |
| ESO 481- G 029  | S0    | 0.48  | 1.16  | 8.91  | –     | < 20  | < 0.06 |
| ESO 418- G 008  | SBd   | 0.48  | 1.22  | 8.92  | 3.9   | 20.40 | 0.15   |
| NGC 1357        | SAab  | 0.93  | 4.67  | 9.38  | 4.4   | 20.45 | 0.17   |
| NGC 1371        | SABa  | 0.20  | 1.36  | 8.80  | 15.8  | 21.00 | 0.59   |
| NGC 1398        | SBab  | 1.14  | 8.96  | 9.60  | 29.0  | 21.27 | 1.09   |
| NGC 1425        | SAb   | 1.08  | 5.89  | 9.47  | 26.6  | 21.23 | 1.00   |
| NGC 1421        | SABbc | 8.48  | 21.32 | 10.16 | 114.5 | 21.86 | 4.30   |
| MCG -02-10-009  | Sc    | 0.53  | 2.13  | 9.07  | –     | < 20  | < 0.06 |
| MCG -03-10-042  | SABbc | 0.86  | 3.40  | 9.28  | 9.1   | 20.76 | 0.34   |
| J034559-1231    | ?     | 0.63  | 1.68  | 9.05  |       | < 20  | < 0.06 |
| MCG -03-10-045  | IBm   | 4.77  | 7.88  | 9.83  | 22.6  | 21.16 | 0.85   |
| NGC 1461        | SA0   | 0.08  | 0.31  | 8.24  | –     | < 20  | < 0.06 |
| UGCA 085        | Sc    | 0.24  | 0.93  | 8.72  | –     | < 20  | < 0.06 |
| NGC 1464        | ?     | 2.61  | 4.89  | 9.59  | 21.1  | 21.13 | 0.79   |
| NGC 1482        | SA0   | 31.95 | 45.32 | 10.63 | 243   | 22.19 | 9.12   |
| IC 2007         | SBc   | 1.28  | 2.77  | 9.31  | 5.6   | 20.55 | 0.21   |
| NGC 1518        | SBdm  | 2.16  | 6.55  | 9.61  | 32.3  | 21.31 | 1.21   |
| NGC 1519        | SBb   | 0.91  | 2.48  | 9.21  | –     | < 20  | < 0.06 |
| ESO 483- G 013  | SA0   | 0.39  | 1.08  | 8.85  | 2.0   | 20.11 | 0.08   |
| J041343-1729    | ?     | 0.98  | 1.77  | 9.16  |       | < 20  | < 0.06 |
| ESO 550- G 008  | E?    | 0.17  | –     | 8.17  | –     | < 20  | < 0.06 |
| UGCA 061        | SBm   | 0.19  | –     | 8.22  | –     | < 20  | < 0.06 |
| IRAS 03007-1531 | ?     | 0.36  | –     | 8.50  | –     | < 20  | < 0.06 |

**Table 3.** Galaxies studied with the GMRT

| Name          | Type  | q     | $S_{60\mu}/S_{100\mu}$ | Comments          |
|---------------|-------|-------|------------------------|-------------------|
| NGC 1407      | E     | 0.45  | 0.29                   | AGN, radio-excess |
| NGC 1371      | Sa    | 1.8   | 0.15                   | AGN, radio-excess |
| NGC 1415      | SB0/a | 2.5   | 0.41                   | normal            |
| NGC 1482      | S0/a  | 2.3   | 0.70                   | star-burst        |
| NGC 1385      | SBcd  | 2.1   | 0.47                   | star-burst        |
| NGC 1377      | S0    | > 3.9 | 1.26                   | radio-deficient   |
| IC 1953       | SBcd  | 3.1   | 0.75                   | radio-deficient   |
| NGC 1309      | Sbc   | 1.95  | 0.37                   | normal            |
| NGC 1345      | Sbc   | 2.43  | 0.49                   | normal            |
| ESO 548-G 036 | S?    | 2.08  | –                      | normal            |